# Dissociation of Molecular Oxygen in the Schumann-Runge Bands

J. E. FREDERICK AND R. D. HUDSON

*Laboratory for Planetary Atmospheres, NASA/Goddard Space Flight Center, Greenbelt, MD 20771*

(Manuscript received 12 October 1979, in final form 15 January 1980)

ABSTRACT

Oscillator strengths and predissociation linewidths deduced in recent studies predict a dissociation rate for $O_2$ in the Schumann-Runge bands which is significantly larger in the upper stratosphere and lower mesosphere than previously believed. Error bars on molecular parameters required in the cross-section calculation translate into uncertainties in the dissociation rate which are less than ±10% at all altitudes where the Schumann-Runge bands are aeronomically significant.

## 1. Introduction

The growing number of measurements of atmospheric composition obtained by satelliteborne remote sensors and *in situ* methods will soon allow better tests of theoretical predictions than has been possible in the past. Therefore, it becomes increasingly important to evaluate the uncertainties in model results due to errors inherent in the input quantities. A long-standing computational difficulty in aeronomy concerns the penetration of photons in the spectral region of the Schumann-Runge (SR) bands of molecular oxygen, 175–205 nm (i.e., Kockarts, 1971; Park, 1974). This paper presents results of a study of the dissociation of $O_2$ in the SR bands based on the molecular parameters derived from laboratory absorption spectra by Frederick and Hudson (1979a). The error bars on rotational linewidths and band oscillator strengths deduced by these authors translate into uncertainty in the dissociation rate of $O_2$ and other constituents which absorb in the SR band spectral region. For example, Frederick and Hudson (1979b) have shown that the potential error in the opacity due to $O_2$ leads to a factor of 2–3 uncertainty in the dissociation rate of NO in the upper stratosphere. Although the present work tabulates values of the dissociation rate of $O_2$ for use in photochemical calculations, these results should not be adopted without due attention to the error bars, which are discussed in detail. Such consideration is essential if comparisons between measurements and theory are to be meaningful.

Data concerning the absorption by $O_2$ in the SR bands have been available for many years (Hudson and Carter, 1968; Ackerman *et al.*, 1970; Hudson and Mahle, 1972) and these results have been used routinely in aeronomic calculations (i.e., Kockarts, 1971; Park, 1974; Blake, 1979). The molecular inputs on which this new study is based are improvements over those previously available. First, as has been discussed by Frederick and Hudson (1979a), the photographic method of recording absorption spectra used by Ackerman *et al.* (1970) causes a large overestimate of rotational linewidths. This leads to a significant underestimate of the $O_2$ dissociation rate in the SR bands below 60 km. Second, the derivation of SR band oscillator strengths and predissociation line widths from laboratory data, as done by Hudson and Mahle (1972), requires use of a detailed theoretical model of the cross section. The model used by Frederick and Hudson (1979a) contains a number of improvements over that used by Hudson and Mahle (1972) and yields results somewhat different from the older study of the same data set. Frederick and Hudson (1979a) give details of the data interpretation.

## 2. Cross-section calculation

Hudson and Carter (1968) and Hudson *et al.* (1969) pointed out the aeronomic significance of the predissociation of $O_2$. Absorption of solar photons excites the stable $B\ ^3\Sigma$ term which undergoes a radiationless transition to a repulsive state with near unit efficiency. Since the upward transition connects two bound states, the cross section displays a complex rotational line structure. The predissociation provides the major source of atomic oxygen in portions of the earth's mesosphere and is non-negligible in the upper stratosphere due to the small cross-section values which exist between absorption lines. A calculation of the $O_2$ absorption cross section in the SR bands requires the following inputs: 1) the wavenumbers $\nu_0$ of all absorption lines, 2) the oscillator strength $f$ of each vibrational band, 3) the width $\Delta L$ in wavenumbers of each rotational

TABLE 1. Oscillator strengths used in the cross-section calculation.

| Band $(v'-v'')$ | Oscillator strength $f(v'-v'')$* | Range of $f(v'-v'')$ |
|---|---|---|
| 2–0 | 2.77 − 8 | (2.72–2.84) − 8 |
| 3–0 | 7.51 − 8 | (7.42–7.64) − 8 |
| 4–0 | 3.04 − 7 | (3.01–3.06) − 7 |
| 5–0 | 7.39 − 7 | (6.84–8.29) − 7 |
| 6–0 | 1.62 − 6 | (1.59–1.67) − 6 |
| 7–0 | 3.15 − 6 | (3.08–3.25) − 6 |
| 8–0 | 5.78 − 6 | (5.74–5.82) − 6 |
| 9–0 | 1.04 − 5 | (8.41–14.0) − 6 |
| 10–0 | 2.60 − 5 | (2.40–3.07) − 5 |
| 11–0 | 1.80 − 5 | (1.72–2.33) − 5 |
| 12–0 | 2.09 − 5 | (2.01–2.17) − 5 |
| 13–0 | 2.69 − 5 | (2.49–3.05) − 5 |
| 14–0 | 3.25 − 5 | — |
| 15–0 | 3.18 − 5 | — |
| 16–0 | 2.93 − 5 | — |
| 17–0 | 2.56 − 5 | — |
| 18–0 | 2.09 − 5 | — |
| 19–0 | 1.60 − 5 | — |

* Best estimates of $f$ from Frederick and Hudson (1979a) through 13–0. Values from Allison *et al.* (1971) for 14–0 through 19–0. Read 2.77 − 8 as $2.77 \times 10^{-8}$.

line, and 4) a line shape which accounts for both Doppler and predissociation broadening. We consider each of these quantities below.

The rotational lines in the SR bands are triplets which, in many cases, have not been resolved in the laboratory. Brix and Herzberg (1954) tabulated positions of the more intense lines and we use these measurements to specify the $F_2$ component of each triplet. The triplet splitting constants deduced by Bergeman and Wofsy (1972) then fix the $F_1$ and $F_3$ positions. Wavenumbers of forbidden lines and lines of the $v'-1$ bands and of the weak $Q$ branches must be computed from theoretical expressions using band constants tabulated by Frederick and Hudson (1979a). The predissociation linewidths deduced from laboratory data are sensitive to the adopted triplet splitting constants. The values of Bergeman and Wofsy (1972) differ significantly from those used in the analysis of Hudson and Mahle (1972) and this accounts for much of the difference between these early SR band molecular parameters and the newer results, even though both are based on the same absorption spectra.

Oscillator strengths for the 2–0 through 13–0 SR bands have been reported by Frederick and Hudson (1979a) together with error bars based on a careful analysis of the absorption spectra originally reported in part by Hudson and Carter (1968) and later by Hudson and Mahle (1972). The overall good agreement between the experimental results and the theoretical calculations of Allison *et al.* (1971) led us to adopt these values for the 14–0 through 19–0 bands. In this region of the spectrum, lines of adjacent bands overlap severely and make a determination of oscillator strengths highly uncertain. Also, we use the results of Allison *et al.* (1971) to describe all absorptions out of the $v'' = 1$ level of $O_2$. Table 1 summarizes the oscillator strengths used in the dissociation rate calculations.

The finite widths of rotational lines in the SR bands results from both Doppler and predissociation broadening with the latter effect usually being dominant. The half-width $\Delta L$ of a rotational line at half-maximum due to predissociation depends only on the upper state $B\ ^3\Sigma$ and its interaction with the repulsive state. The shape of the plot $\Delta L(v')$ vs $v'$ obtained by Frederick and Hudson (1979a) is consistent with a single repulsive curve intersecting the $B\ ^3\Sigma$ potential well near $v' = 4$. Error bars on the $\Delta L$ values tend to be large since most of the widths are comparable to or smaller than the resolution of instruments used to date. The deduction of linewidths must therefore be done indirectly using methods described by Frederick and Hudson (1979a) whose values with error bars appear in Table 2. For the 14–0 through 19–0 bands we adopt the linewidths given by Hudson and Mahle (1972).

The cross section of a rotational line integrated over wavenumber $\nu$ is

$$\int \sigma(\nu)d\nu = \frac{\pi e^2}{mc^2} f(v',v'') \frac{S(J',J'')}{2J''+1},$$

TABLE 2. Predissociation line widths used in the cross-section calculation.

| Upper state vibrational level $v'-0$ | Predissociation line width $(cm^{-1})$* | Range of line widths $(cm^{-1})$ |
|---|---|---|
| 2–0 | 1.21 − 1 | (1.14–1.32) − 1 |
| 3–0 | 9.20 − 1 | (8.80–9.58) − 1 |
| 4–0 | 2.09 + 0 | (2.04–2.13) + 0 |
| 5–0 | 1.17 + 0 | (1.00–1.46) + 0 |
| 6–0 | 5.56 − 1 | (4.85–6.56) − 1 |
| 7–0 | 8.52 − 1 | (7.96–9.32) − 1 |
| 8–0 | 7.17 − 1 | (6.14–7.76) − 1 |
| 9–0 | 3.79 − 1 | (2.07–6.02) − 1 |
| 10–0 | 2.11 − 1 | (1.65–2.34) − 1 |
| 11–0 | 6.35 − 1 | (4.00–8.60) − 1 |
| 12–0 | 4.06 − 1 | (3.75–4.40) − 1 |
| 13–0 | 6.60 − 2 | (5.90–7.20) − 2 |
| 14–0 | 3.0 − 2 | — |
| 15–0 | 1.0 − 1 | — |
| 16–0 | 1.3 − 1 | — |
| 17–0 | 2.0 − 1 | — |
| 18–0 | 2.0 − 1 | — |
| 19–0 | 2.0 − 1 | — |

* Reported values are predissociation half-widths at half-maximum. Results through 13–0 are from Frederick and Hudson (1979a). For 14–0 through 19–0 the values are from Hudson and Mahle (1972).

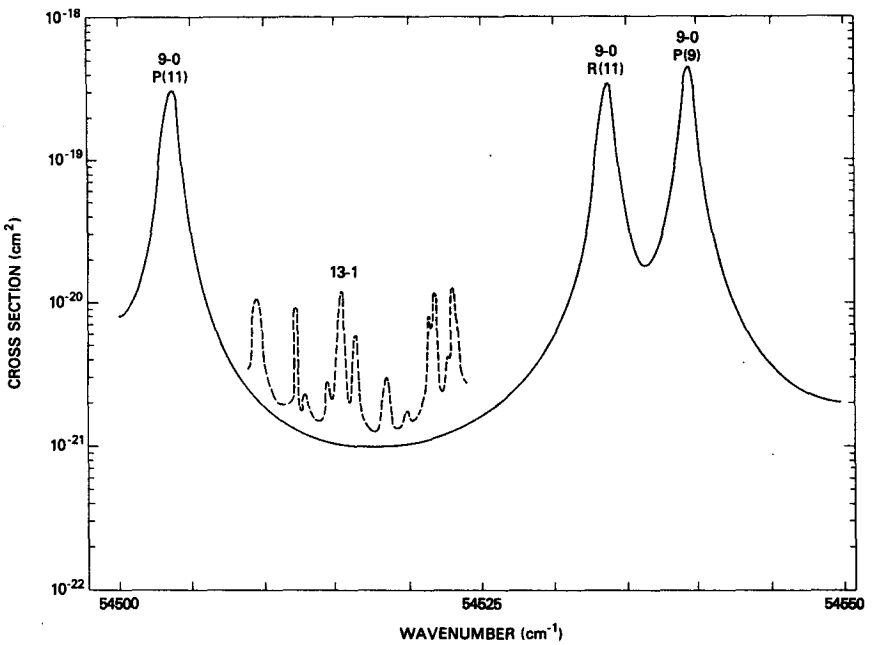


FIG. 1. Cross section in a portion of the 9–0 Schumann-Runge band. Solid line refers to a temperature of 200 K. Dashed line shows appearance of the 13–1 band at 300 K.

where $f$ is the oscillator strength for band $v'v''$, $S(J',J'')$ the rotational line strength for a transition from lower state $J''$ to $J'$ (Tatum, 1966), $c$ the speed of light, and $e$ and $m$ are the charge and mass of the electron, respectively. The combined effects of predissociation and Doppler broadening lead to a line shape described by the Voigt profile (Goody, 1964). The cross section at a given wavenumber consists of the sum of contributions from wings of all lines throughout the SR bands. Although a large portion comes from lines in the immediate vicinity, the sum of thousands of individual contributions from line wings whose centers are far removed can be of comparable size and must be included to obtain accurate cross sections between the peaks.

For the cross-section calculation we divided the spectral region from 48 600 through 57 000 $cm^{-1}$ into intervals of width 25 $cm^{-1}$. Within each interval a wavenumber grid was chosen based on the widths of rotational lines that lie in it so as to assure that all finestructure was resolved. The grid spacing ranged from $2.0 \times 10^{-2}$ $cm^{-1}$ up to $2.5 \times 10^{-1}$ $cm^{-1}$. To allow for temperature variations the calculations were performed at 150, 200, 250 and 300 K. The continuum cross section that underlies the SR bands becomes significant at low altitudes since in some cases it is comparable to the contribution from overlapping line wings. We have adopted the temperature dependent values of Hudson and Mahle (1972) for this purpose. Absorption out of the $v'' = 1$ level is the major cause of temperature dependence in the SR band cross section. Allison *et al.* (1971) show that oscillator strengths for the $v'-1$ bands are much larger than those for $v'-0$ transitions. The sensitive temperature-dependence of the $v'' = 1$ population then gives an increasing cross section with increasing temperature.

Fig. 1 illustrates the behavior of the cross section at a temperature of 200 K (solid line) in the 9–0 band. The maxima corresponding to the $P(11)$, $R(11)$ and $P(9)$ rotational lines are actually triplets whose separations lie in the range 0.15–0.25 $cm^{-1}$. Since the predissociation half-width here is 0.38 $cm^{-1}$ the components are not distinguishable. Between the lines the cross section falls to a value of order $10^{-21}$ $cm^2$ which results from the broad wings of a Voigt profile. The underlying continuum cross section is of order $1 \times 10^{-22}$ $cm^2$ in this spectral region (Hudson and Mahle, 1972). The dashed line in Fig. 1 gives the cross section at a temperature of 300 K. Absorption in the 13–1 band becomes significant here and greatly alters the values between the 9–0 band peaks. In practice the $v'-1$ bands do not make a large contribution to the total cross section until the temperature approaches 300 K so that their effects throughout the stratosphere and mesosphere are minor.

## 3. Dissociation rates

The dissociation rate calculation adopts the solar irradiance data of Brueckner *et al.* (1976) and the

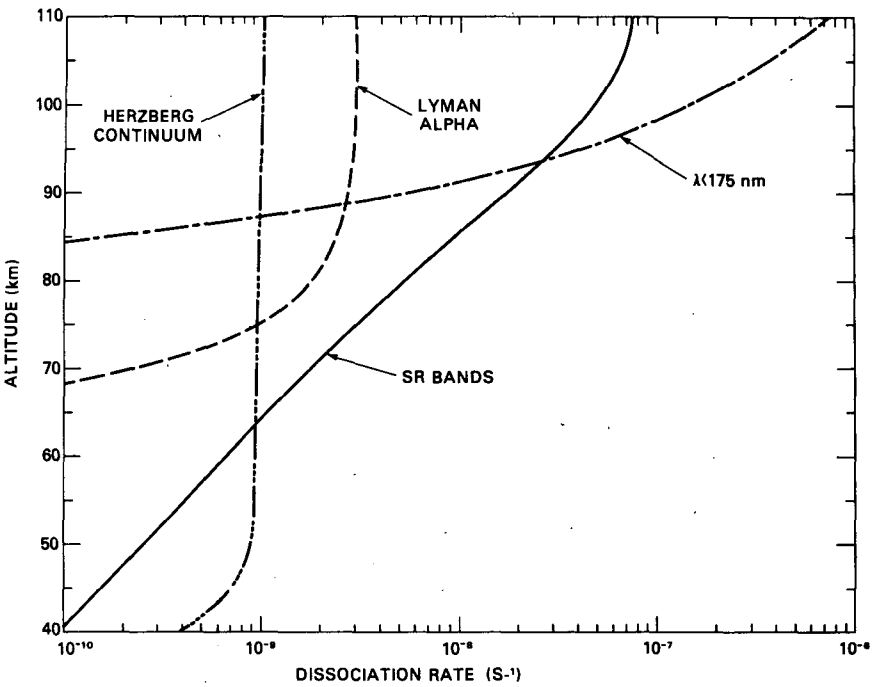


FIG. 2. Dissociation rates of $O_2$ due to various spectral regions for an overhead sun, 40–110 km.

temperature profile of the *U.S. Standard Atmosphere, 1976*. Opacity due to ozone should be included as of the lower mesosphere and we therefore report results in a form which allows use of an arbitrary ozone model. We express the total SR band dissociation rate as

$$J(\mathrm{SR}) = \sum_{i=1}^{17} J(i) \exp\{-\tau_i(O_3)\}, \qquad (1)$$

where $\tau_i(O_3)$ is the slant path optical depth due to $O_3$ and $J(i)$ includes only the $O_2$ opacity for a spectral bandwidth $i$, i.e.,

$$J(i) = \int_{\lambda(i)}^{\lambda(i)+\Delta\lambda} d\lambda \phi(\lambda)\sigma(\lambda) \exp\{-\tau(O_2,\lambda)\}. \qquad (2)$$

The computed $O_2$ cross section is $\sigma(\lambda)$ at wavelength $\lambda$, $\phi(\lambda)$ is the solar irradiance and $\tau(O_2,\lambda)$ the optical depth due to molecular oxygen. The 17 intervals to which the $J(i)$ refer cover the range 48 600–57 000 $cm^{-1}$ in 500 $cm^{-1}$ segments (except for $i = 1$ which extends from 48 600 to 49 000 $cm^{-1}$). This matches the grid on which Ackerman (1971) reported $O_3$ cross sections so that $\tau_1(O_3)$ is readily computed for a given model profile for use in Eq. (1). The Appendix presents numerical values of the dissociation rate as a function of $O_2$ column density for use in photochemical models. For $O_2$ columns less than $5 \times 10^{20}$ $cm^{-2}$ the effects of $O_3$ opacity are negligible and we tabulate only the total $J(\mathrm{SR})$. For larger $O_2$ columns we present the individual $J(i)$, $i = 1, 17$.

Figs. 2 and 3 present the SR band dissociation rate and compare it with dissociation in other spectral regions. The results shown are based on the best estimate cross sections of Frederick and Hudson (1979a) with $O_3$ opacity based on the profile of Krueger and Minzner (1976). For wavelengths above and below the Schumann-Runge bands we adopt the $O_2$ cross sections of Ackerman (1971). We use the solar irradiance tabulation of Nicolet (1975) in the Herzberg continuum and the data of Heroux and Swirbalus (1976) multiplied by 1.1 for wavelengths < 175 nm. Fig. 2, for an overhead sun, shows that $J(\mathrm{SR})$ is the largest single contribution between 64 and 94 km but is non-negligible throughout the 40–100 km region. Fig. 3 shows that in the middle and upper stratosphere the Herzberg continuum ($\lambda > 205$ nm) is responsible for more dissociation than the SR bands; however, the two wavelength regions provide comparable contributions. Fig. 4 presents $J(\mathrm{SR})$ as a fraction of the total $O_2$ dissociation rate for an overhead sun. The SR bands account for more than 15% of the total dissociation at all altitudes from 105 km to the lower stratosphere. Due to the rapid attenuation of the Herzberg continuum the SR bands become rela-

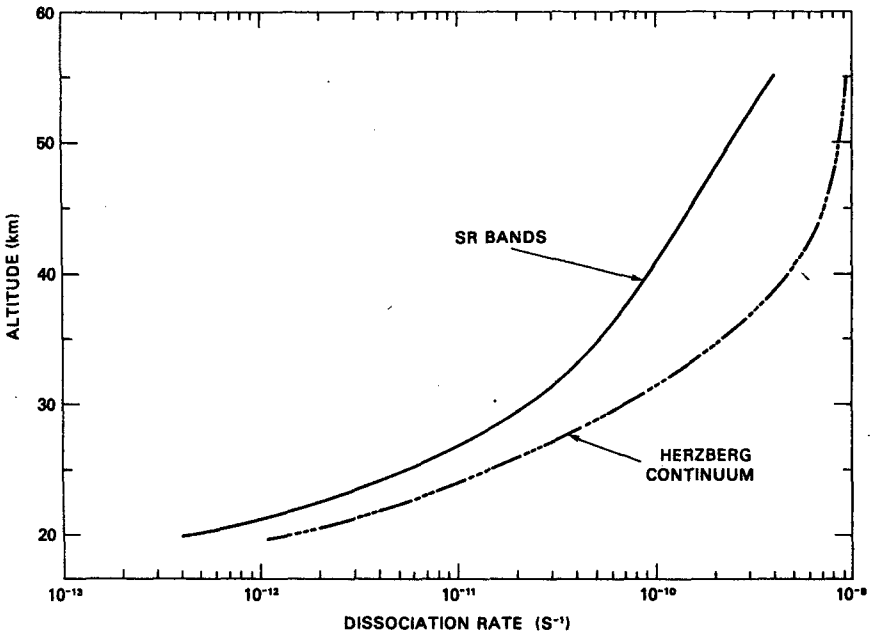


FIG. 3. Dissociation rates of $O_2$ due to the Schumann-Runge bands and the Herzberg continuum ($\lambda > 205$ nm) in the stratosphere. Ozone opacity is included as discussed in the text. The sun is overhead.

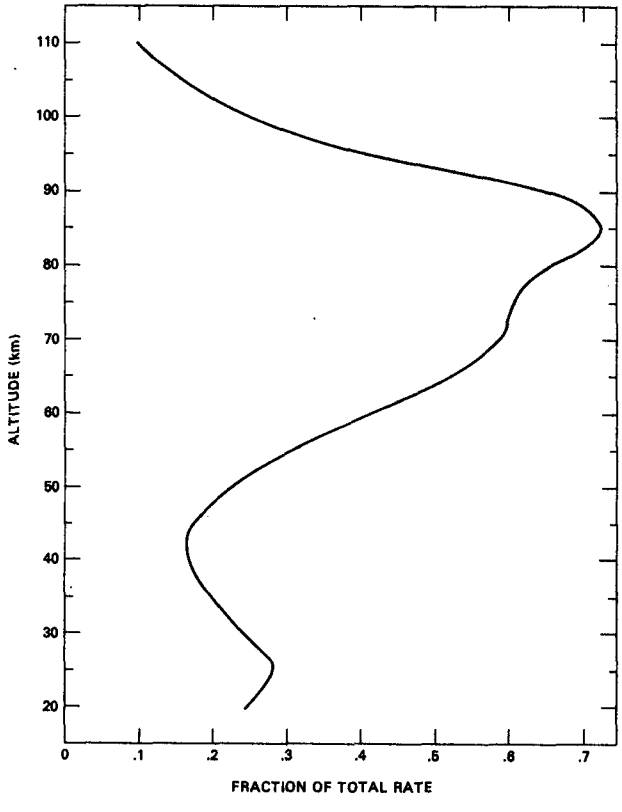


FIG. 4. Dissociation rate of $O_2$ in the Schumann-Runge bands expressed as a fraction of the total dissociation rate. The sun is overhead.

tively more important between 20 and 30 km than they are immediately below the stratopause.

Park (1974) computed the dissociation rate of $O_2$ in the SR bands based on the molecular parameters of Ackerman *et al.* (1970). As discussed by Frederick

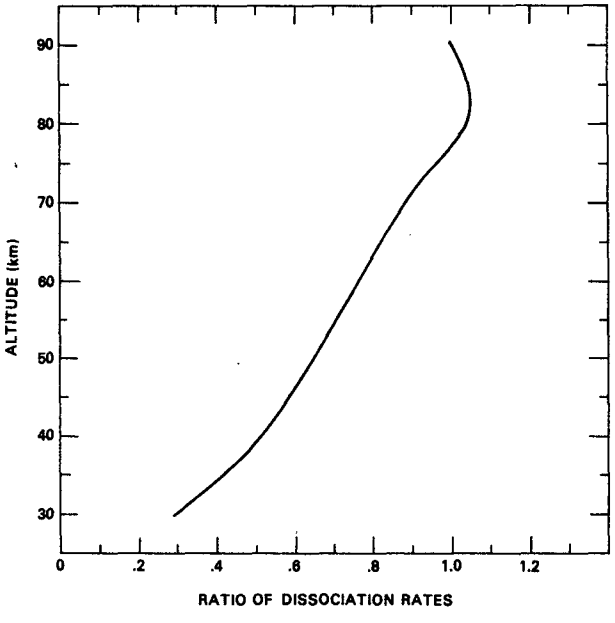


FIG. 5. Ratio of the Schumann-Runge band dissociation rate computed by Park (1974) to that computed in the present work. The sun is overhead.

and Hudson (1979a) the newer linewidths are smaller than previously believed and this allows more solar photons to penetrate to low altitudes than predicted by earlier calculations. Essentially all of the incident irradiance in the 175–205 nm regions is absorbed by $O_2$. Hence, the atomic oxygen production rate is fixed by the number of photons incident on the atmosphere and not by the magnitude of the $O_2$ cross section. The effect of the smaller rotational line widths is to alter the shape of the atomic oxygen production profile but not the integrated magnitude. Fig. 5 presents the ratio of the $J$(SR) results of Park (1974) to those computed here for an overhead sun. Both calculations include the small continuum cross section which underlines the bands. The older values have been normalized to those of the present work at 90 km to account for the difference in solar irradiances used. Values in use today are a factor of 1.6–1.7 smaller than those accepted several years ago (Ackerman, 1971; Brueckner *et al.*, 1976). At the stratopause, for an overhead sun, the new $J$(SR) value is a factor of 1.5 larger than predicted by the Ackerman *et al.* (1970) line widths and this difference increases to 1.9–2.0 by 40 km. We note that the calculations of Park (1974) assumed a Lorentzian line shape whereas the new results are based on a Voigt profile. This makes a minor contribution to the differences between results since the wings of the Voigt profile are Lorentzian.

## 4. Error analysis

Frederick and Hudson (1980) have shown that the uncertainty in the transmission of solar irradiance due to error bars on the SR band cross sections increases with decreasing altitude roughly as the $O_2$ column abundance. A similar analysis carried out for the dissociation rate of $O_2$ shows that this quantity is much less sensitive to cross section uncertainties than are the transmission functions. The SR band dissociation rate per unit wavelength is

$$j = \sigma(\lambda)\phi(\lambda)\exp\{-\tau(O_2,\lambda) - \tau(O_3,\lambda)\},$$

where $\tau(s,\lambda)$ is the slant path optical depth at wavelength $\lambda$ due to gas $s$. For purposes of illustration we neglect the temperature dependence in the $O_2$ cross section and write

$$\tau(O_2,\lambda) = \sigma(\lambda)N(O_2),$$

where $N(O_2)$ is the column density above the level concerned measured along the solar beam. A small uncertainty $\Delta\sigma(\lambda)$ in the cross section leads to a corresponding uncertainty in $j$ of

$$\frac{\Delta j}{j} = \{1 - \sigma(\lambda)N(O_2)\}\frac{\Delta\sigma(\lambda)}{\sigma(\lambda)}.$$

At an optical depth of unity, small errors in the cross section have no impact on the computed dissociation rate while at small $O_2$ columns the error is proportional to $\Delta\sigma$. It is only at large optical depths, $\sigma(\lambda)N(O_2) \gg 1$, that small cross section errors have a significant impact on $J$(SR).

In order to assess the uncertainty in the $O_2$ dissociation rate in the SR bands we have generated three sets of cross sections. The best estimates are based on the oscillator strengths and linewidths of Frederick and Hudson (1979a) while the error bars on these quantities define upper and lower limits for the cross section. The error bars on the $f$ and $\Delta L$ values are not independent. The fitting procedure used by Frederick and Hudson (1979a) gives more accurate values of the product $f\Delta L$ than either quantity alone, and in the line wings the cross section is proportional to this product. The upper limits of $f$ in Table 1 are associated with the lower limits of the corresponding $\Delta L$. Near the peaks in the cross section the values are nearly independent of $\Delta L$ and the uncertainty in $J$(SR) here reflects that in the oscillator strengths which is often less than $\pm 10\%$. In the minima between rotational lines the cross section is proportional to the product $f\Delta L$. From the discussion above, the uncertainty in this product is much less than if the error bars on $f$ and $\Delta L$ were additive.

We have computed SR band dissociation rate profiles using cross sections which represent upper and lower limits defined by the error bars of Table 1 and 2. The results for the overhead sun dissociation rate at 90 km lie between 0.93 and 1.09 times the best estimate tabulated in the Appendix. At 60 km and below the extreme cases are within $\pm 5\%$ of the preferred values. At a given altitude the wavelengths which provide the bulk of the SR band odd oxygen production are optically thin and are therefore rather insensitive to small variations in the cross section. Large changes in the linewidths are required to cause major changes in the computed dissociation rate, as in the case in the comparison of Fig. 5.

## 5. Conclusion

Recent molecular data concerning absorption by $O_2$ in the 175–205 nm region imply a significantly larger dissociation rate in the SR bands than is included in current aeronomic models of the upper stratosphere and lower mesosphere. Error bars on the dissociation rates are less than $\pm 10\%$ due to cross section uncertainties, while the solar irradiance is likely known to $\pm 20\%$. Frederick *et al.* (1978) suggested that an enhanced production rate of odd oxygen near the stratopause would aid in reconciling photochemical theories and available data. The results obtained here support the validity of this speculation.

APPENDIX

## Tabulation of Dissociation Rates of Molecular Oxygen in the Schumann-Runge Bands

TABLE A1. Spectral intervals for which dissociation rates are reported when $O_3$ opacity is significant.

| Label ($i$) | Wavenumber range ($cm^{-1}$) |
|---|---|
| 1 | 48 600–49 000 |
| 2 | 49 000–49 500 |
| 3 | 49 500–50 000 |
| 4 | 50 000–50 500 |
| 5 | 50 500–51 000 |
| 6 | 51 000–51 500 |
| 7 | 51 500–52 000 |
| 8 | 52 000–52 500 |
| 9 | 52 500–53 000 |
| 10 | 53 000–53 500 |
| 11 | 53 500–54 000 |
| 12 | 54 000–54 500 |
| 13 | 54 500–55 000 |
| 14 | 55 000–55 500 |
| 15 | 55 500–56 000 |
| 16 | 56 000–56 500 |
| 17 | 56 500–57 000 |

TABLE A2. Dissociation rate of $O_2$ in the Schumann-Runge bands at column densities where $O_3$ opacity is negligible.

| $O_2$ Column density ($cm^{-2}$) | $Z_0$* (km) | Dissociation rate ($s^{-1}$) |
|---|---|---|
| 1.555 + 17** | 110 | 7.76 − 8 |
| 3.901 + 17 | 105 | 6.66 − 8 |
| 1.060 + 18 | 100 | 4.96 − 8 |
| 2.905 + 18 | 95 | 3.12 − 8 |
| 7.710 + 18 | 90 | 1.78 − 8 |
| 1.960 + 19 | 85 | 9.54 − 9 |
| 4.716 + 19 | 80 | 5.31 − 9 |
| 1.078 + 20 | 75 | 3.04 − 9 |
| 2.358 + 20 | 70 | 1.80 − 9 |
| 4.939 + 20 | 65 | 1.09 − 9 |

* Altitude corresponding to the given $O_2$ column density for an overhead sun.

** Read 1.555 + 17 as $1.555 \times 10^{17}$.

TABLE A3. Dissociation rate of $O_2$ in the Schumann-Runge bands at column densities where $O_3$ opacity should be included.

| $O_2$ column density ($cm^{-2}$) | $Z_0$ (km) | $J$ ($i$ = 1)* ($s^{-1}$) | $J$ ($i$ = 2) ($s^{-1}$) | $J$ ($i$ = 3) ($s^{-1}$) |
|---|---|---|---|---|
| 9.919 + 20 | 60 | 1.66 − 11 | 1.80 − 11 | 1.51 − 11 |
| 1.919 + 21 | 55 | 1.65 − 11 | 1.79 − 11 | 1.52 − 11 |
| 3.607 + 21 | 50 | 1.62 − 11 | 1.76 − 11 | 1.51 − 11 |
| 6.756 + 21 | 45 | 1.55 − 11 | 1.68 − 11 | 1.43 − 11 |
| 1.299 + 22 | 40 | 1.44 − 11 | 1.54 − 11 | 1.28 − 11 |
| 2.595 + 22 | 35 | 1.23 − 11 | 1.30 − 11 | 1.06 − 11 |
| 5.382 + 22 | 30 | 8.73 − 12 | 9.07 − 12 | 7.26 − 12 |
| 1.145 + 23 | 25 | 4.17 − 12 | 4.17 − 12 | 3.20 − 12 |
| 2.480 + 23 | 20 | 8.24 − 13 | 7.57 − 13 | 5.34 − 13 |

TABLE A3. (*Continued*)

| $O_2$ column density ($cm^{-2}$) | $J$ ($i$ = 4) ($s^{-1}$) | $J$ ($i$ = 5) ($s^{-1}$) | $J$ ($i$ = 6) ($s^{-1}$) |
|---|---|---|---|
| 9.919 + 20 | 1.54 − 11 | 2.87 − 11 | 6.15 − 11 |
| 1.919 + 21 | 1.58 − 11 | 2.48 − 11 | 4.56 − 11 |
| 3.607 + 21 | 1.57 − 11 | 2.17 − 11 | 3.28 − 11 |
| 6.756 + 21 | 1.39 − 11 | 1.71 − 11 | 2.11 − 11 |
| 1.299 + 22 | 1.14 − 11 | 1.25 − 11 | 1.24 − 11 |
| 2.595 + 22 | 8.95 − 12 | 8.62 − 12 | 6.74 − 12 |
| 5.382 + 22 | 5.76 − 12 | 4.84 − 12 | 2.94 − 12 |
| 1.145 + 23 | 2.35 − 12 | 1.69 − 12 | 7.60 − 13 |
| 2.480 + 23 | 3.47 − 13 | 2.00 − 13 | 5.94 − 14 |

| $O_2$ column density ($cm^{-2}$) | $J$ ($i$ = 7) ($s^{-1}$) | $J$ ($i$ = 8) ($s^{-1}$) | $J$ ($i$ = 9) ($s^{-1}$) |
|---|---|---|---|
| 9.919 + 20 | 7.65 − 11 | 6.59 − 11 | 5.92 − 11 |
| 1.919 + 21 | 4.76 − 11 | 4.85 − 11 | 4.13 − 11 |
| 3.607 + 21 | 2.87 − 11 | 3.29 − 11 | 2.69 − 11 |
| 6.756 + 21 | 1.44 − 11 | 1.76 − 11 | 1.39 − 11 |
| 1.299 + 22 | 6.50 − 12 | 8.32 − 12 | 6.16 − 12 |
| 2.595 + 22 | 2.82 − 12 | 3.59 − 12 | 2.45 − 12 |
| 5.382 + 22 | 1.05 − 12 | 1.10 − 12 | 6.84 − 13 |
| 1.145 + 23 | 2.28 − 13 | 1.52 − 13 | 7.81 − 14 |
| 2.480 + 23 | 1.32 − 14 | 3.75 − 15 | 1.14 − 15 |

| $O_2$ column density ($cm^{-2}$) | $J$ ($i$ = 10) ($s^{-1}$) | $J$ ($i$ = 11) ($s^{-1}$) | $J$ ($i$ = 12) ($s^{-1}$) |
|---|---|---|---|
| 9.919 + 20 | 7.24 − 11 | 6.62 − 11 | 5.40 − 11 |
| 1.919 + 21 | 4.28 − 11 | 3.62 − 11 | 2.58 − 11 |
| 3.607 + 21 | 2.22 − 11 | 1.50 − 11 | 9.72 − 12 |
| 6.756 + 21 | 9.29 − 12 | 3.95 − 12 | 2.45 − 12 |
| 1.299 + 22 | 3.42 − 12 | 7.81 − 13 | 4.30 − 13 |
| 2.595 + 22 | 1.07 − 12 | 1.12 − 13 | 4.35 − 14 |
| 5.382 + 22 | 1.78 − 13 | 4.83 − 15 | 7.88 − 16 |
| 1.145 + 23 | 6.62 − 15 | 1.03 − 17 | 2.73 − 19 |
| 2.480 + 23 | 1.02 − 17 | 2.57 − 23 | 1.52 − 26 |

| $O_2$ column density ($cm^{-2}$) | $J$ ($i$ = 13) ($s^{-1}$) | $J$ ($i$ = 14) ($s^{-1}$) | $J$ ($i$ = 15) ($s^{-1}$) |
|---|---|---|---|
| 9.919 + 20 | 4.70 − 11 | 2.54 − 11 | 2.63 − 11 |
| 1.919 + 21 | 1.89 − 11 | 5.88 − 12 | 5.04 − 12 |
| 3.607 + 21 | 5.44 − 12 | 6.68 − 13 | 2.46 − 13 |
| 6.756 + 21 | 7.93 − 13 | 2.33 − 14 | 1.34 − 15 |
| 1.299 + 22 | 5.36 − 14 | 1.91 − 16 | 4.78 − 19 |
| 2.595 + 22 | 1.09 − 15 | 1.01 − 19 | 1.42 − 24 |
| 5.382 + 22 | 1.02 − 18 | 8.10 − 26 | 7.93 − 35 |
| 1.145 + 23 | 8.09 − 25 | 4.70 − 38 | 1.96 − 55 |
| 2.480 + 23 | 1.01 − 37 | 0 | 0 |

| $O_2$ column density ($cm^{-2}$) | $J$ ($i$ = 16) ($s^{-1}$) | $J$ ($i$ = 17) ($s^{-1}$) |
|---|---|---|
| 9.919 + 20 | 6.84 − 12 | 1.07 − 16 |
| 1.919 + 21 | 4.31 − 13 | 3.31 − 23 |
| 3.607 + 21 | 2.30 − 15 | 2.83 − 36 |
| 6.756 + 21 | 1.66 − 19 | 0 |
| 1.299 + 22 | 2.73 − 26 | 0 |
| 2.595 + 22 | 3.05 − 37 | 0 |
| 5.382 + 22 | 4.42 − 56 | 0 |
| 1.145 + 23 | 0 | 0 |
| 2.480 + 23 | 0 | 0 |

* $J(i)$ = $O_2$ dissociation rate, unattenuated by ozone, for the spectral range $i$ defined in Table A1. The total dissociation rate, including $O_3$ opacity, may be computed from the $J(i)$ by Eq. (1) of the text.

## REFERENCES


Ackerman, M., 1971: Ultraviolet solar radiation related to mesospheric processes. *Mesospheric Models and Related Experiments*, G. Fiocco, Ed., D. Reidel, 149–159.

——, F. Biaume and G. Kockarts, 1970: Absorption cross sections of the Schumann-Runge bands of molecular oxygen. *Planet. Space Sci.*, **18,** 1639–1651.

Allison, A. C., A. Dalgarno and N. W. Pasachoff, 1971: Absorption by vibrationally excited molecular oxygen in the Schumann-Runge continuum. *Planet. Space Sci.*, **19,** 1463–1473.

Bergeman, T. H., and S. C. Wofsy, 1972: The fine structure of $O_2(B^3\Sigma_u)$. *Chem. Phys. Lett.*, **15,** 104–107.

Blake, A. J., 1979: An atmospheric absorption model for the Schumann-Runge bands of oxygen. *J. Geophys. Res.*, **84,** 3272–3282.

Brix, P., and G. Herzberg, 1954: Fine structure of the Schumann-Runge bands near the convergence limit and the dissociation energy of the oxygen molecule. *Can. J. Phys.*, **32,** 110–135.

Brueckner, G. E., J.-D. F. Bartoe, O. Kjeldseth Moe and M. E. Van Hoosier, 1976: Absolute ultraviolet intensities and their variations with solar activity. I. The wavelength region 1750–2100 Å. *Astrophys. J.*, **209,** 935–944.

Frederick, J. E., and R. D. Hudson, 1979a: Predissociation line widths and oscillator strengths for the 2–0 to 13–0 Schumann-Runge bands of $O_2$. *J. Mol. Spectros.*, **74,** 247–256.

——, and ——, 1979b: Predissociation of nitric oxide in the mesosphere and stratosphere. *J. Atmos. Sci.*, **36,** 737–745.

——, and ——, 1980: Atmospheric opacity in the Schumann-Runge bands and the aeronomic dissociation of water vapor. *J. Atmos. Sci.*, **37,** 1084–1094.

——, B. W. Guenther, P. B. Hays and D. F. Heath, 1978: Ozone profiles and chemical loss rates in the tropical stratosphere deduced from backscatter ultraviolet measurements. *J. Geophys. Res.*, **83,** 953–958.

Goody, R. M., 1964: *Atmospheric Radiation* I. *Theoretical Basis*. Clarendon Press, Oxford, 436 pp.

Heroux, L., and R. A. Swirbalus, 1976: Full-disk solar fluxes between 1230 and 1940 Å. *J. Geophys. Res.*, **81,** 436–440.

Hudson, R. D., and V. L. Carter, 1968: Absorption of oxygen at elevated temperatures (300° to 900°K) in the Schumann-Runge system. *J. Opt. Soc. Amer.*, **58,** 1621–1629.

——, and S. H. Mahle, 1972: Photodissociation rates of molecular oxygen in the mesosphere and lower thermosphere. *J. Geophys. Res.*, **77,** 2902–2914.

——, V. L. Carter and E. L. Brieg, 1969: Predissociation in the Schumann-Runge system of $O_2$: Laboratory measurements and atmospheric effects. *J. Geophys. Res.*, **74,** 4079–4086.

Kockarts, G., 1971: Penetration of solar radiation in the Schumann-Runge bands of molecular oxygen. *Mesospheric Models and Related Experiments*, G. Fiocco, Ed., D. Reidel, 160–176.

Krueger, A. J., and R. A. Minzner, 1976: A mid-latitude ozone model for the 1976 U.S. Standard Atmosphere. *J. Geophys. Res.*, **81,** 4477–4481.

Nicolet, M., 1975: Stratospheric ozone: An introduction to its study. *Rev. Geophys. Space Phys.*, **13,** 593–636.

Park, J. H., 1974: The equivalent mean absorption cross section for the $O_2$ Schumann-Runge bands: Application to the $H_2O$ and NO photodissociation rates. *J. Atmos. Sci.*, **31,** 1893–1897.

Tatum, J. B., 1966: Hönl-London factors for $^3\Sigma$–$^3\Sigma$ transitions. *Can. J. Phys.*, **44,** 2944–2946.

*U.S. Standard Atmosphere, 1976*: U.S. Government Printing Office, Washington, DC.